Zeng *et al. Heritage Science (2023) 11:247*
https://doi.org/10.1186/s40494-023-01096-y

Heritage Science

RESEARCH

Open Access

Interregional and intraregional interaction of the Tianshanbeilu population in eastern Xinjiang from the perspective of pottery analysis

Baodong Zeng[1], Tao Ma[2], Yongqiang Wang[3], Jie Zhang[3], Liangren Zhang[1*] and Xi'en Chang[3]

Abstract

The beginning of human settlement in the Hami Basin, located in the eastern part of Xinjiang, has been a focal question for the academic community in China. In particular, the thesis that the immigrating population from the Hexi Corridor since the late Neolithic founded the Tianshanbeilu culture has riveted the attention of scholars. Pottery wares, abundantly discovered at the synonymous cemetery of this culture, have played a key role in extrapolating population migration and cultural interaction. This paper aims to test the thesis by characterizing the chemical composition, painting pigment, and carburizing technique of 70 pottery samples from the cemetery with various scientific methods. It shows that the chemical compositions of the coarse pottery in the three colors of red, yellow, and gray, painted and unpainted alike, are remarkably different from those of fine pottery in black and red, indicating that the raw materials for the coarse and fine pottery samples are possibly procured from different sources; the pigments of the red slip and black paint are derived from hematite, black manganese ore, and carbon black; carburizing and polishing techniques are further applied to the gray coarse pottery; In combination with the compositional data of pottery samples from the Yaer cemetery also in the Hami Basin and the Xichengyi settlement in the Hexi Corridor, this paper finds that some pottery wares of the Tianshanbeilu culture were exchanged within the Hami Basin, but each site had its own production facility. No direct exchange of pottery wares with Xichengyi is attested; the similar style of pottery wares between the two sites may have resulted from population migration and technological exchange.

Keywords Xinjiang, Bronze age, Pottery analysis, Technological exchange, Population migration

Introduction

The Hami Basin, located in eastern Xinjiang, serves as a gateway to Xinjiang from China proper. Far from the Atlantic, Pacific, and Indian Oceans, the climate here is typical of the temperate continental type: hot in summer and cold in winter, with low precipitation yet high evaporation. The basin is dotted with several oases sustained by several rivers fed by snow water from the eastern Tianshan Mountains to the north, the largest of which are the Hami River and the Baiyang River. The oases themselves form a network of mutual interaction and connect to the outside world, to the southeast through the Xingxing Gorge to the Hexi Corridor, to the north through a few passes across the eastern Tianshan Mountains to the Barkol-Yiwu Steppe, and to the west to the Turpan Basin. Due to its unique geographical location, the Hami Basin

*Correspondence:
Liangren Zhang
zhlr@nju.edu.cn
[1] School of History, Nanjing University, 163 Xianlin Blvd, Nanjing 210023, Jiangsu, China
[2] Ningbo Museum, 1000 Shounan Middle Road, Ningbo 315000, Zhejiang, China
[3] Xinjiang Institute of Cultural Relics and Archaeology, 4 South Beijing Road, Urumqi 830011, Xinjiang, China

has been home to different peoples and cultures since ancient times.

The Tianshanbeilu cemetery (Fig. 1) is located in the Hami River oasis, in front of the Hami Railway Station in the south of the city of Hami. Between 1988 and 1997, at the call of road construction, archaeologists excavated over 700 tombs and obtained a great assemblage of artifacts of pottery, metal, stone, bone, and shell. Not all the tombs of this cemetery were excavated; while some were looted prior to the construction, the others, which are located out of the construction zone, were left untouched. Among the numerous and distinctive pottery wares, one-third are painted ones. After the excavation, several scholars have studied the shape, pattern, and chronology of the pottery wares. Lv et al. [1] formulated a four-period chronology out of them and assigned the cemetery to the Bronze Age, roughly nineteenth to thirteenth centuries BC. Based on 41 radiocarbon dates, Tong et al. [2] placed the chronology of the four periods within the range of 2011-1029 BC. Thus, the Tianshanbeilu cemetery overlaps chronologically with the Yanbulak cemetery (1300 BC–565 BC), also in the Hami Basin, by a few hundred years.

Because neither Neolithic nor earlier Bronze Age site has been discovered in the Hami region, the origin of the material culture, particularly the pottery wares and the origin of the population that created it, has been a focal question of Chinese scholars. Shui [3] was the first to identify two typological groups: one associated with the Yanbulak culture, named after the synonymous cemetery, and the other with the Machang and Siba cultures in the Hexi Corridor. Li [4] nevertheless found another two types: one derived from the abovementioned Machang and the Siba cultures, and the other, comprised only of the unique double-ear cylindrical jars, presumed to be from southern Siberia and western Mongolia; most scholars agreed with Li on the origin of the first type but diverged regarding the origin of the other type. While some connected it to the eastward and southward spread of Eurasian steppe cultures, others looked to the contemporary Xiaohe culture in the Tarim desert. Whichever view is valid, we can see that the pottery wares uncovered from the Tianshanbeilu cemetery are rather diverse, multi-sourced, yet distinctive.

The thesis of the origin of the Tianshanbeilu culture has been corroborated by the studies of the other materials. Wang et al. [5] discovered that the Tianshanbeilu population adopted C3 and C4 crops (wheat and millet) and millet from the Hexi Corridor during the westward migration of the Machang and Siba populations.

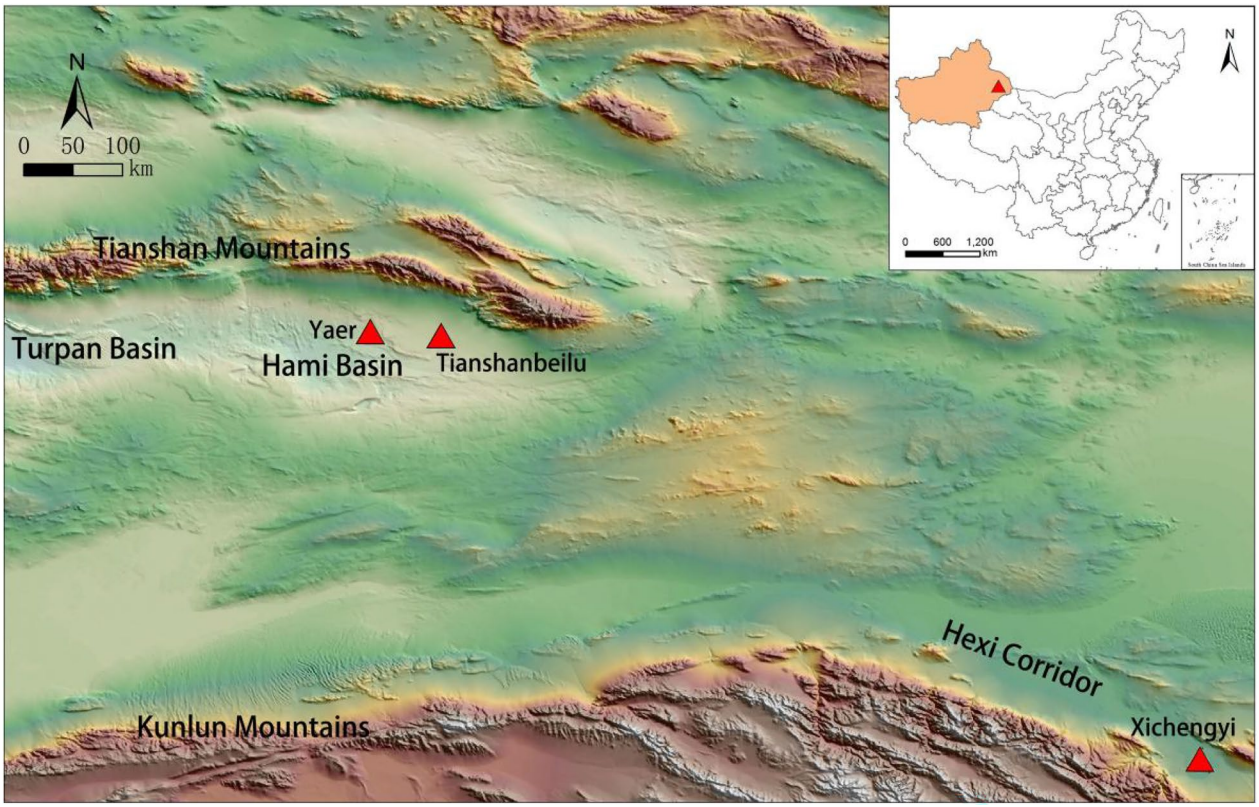

Fig. 1 Location of the Tianshanbeilu Cemetery

Concomitantly, Gao et al. [6] found that the metal artifacts unearthed at the Tianshanbeilu cemetery bespeak the transmission of metallurgy of these populations. The study of lead isotopes and highly radiogenic lead in metal artifacts from the Tianshanbeilu cemetery also reflects population migration [7]. The genetic lineage of the Tianshanbeilu population is related to that of its Machang counterpart in the Hexi Corridor and the ancient population in Siberia [8], which lends strong support to the above-mentioned "immigration" thesis.

Although many typological studies have been conducted on the pottery wares unearthed from the Tianshanbeilu cemetery, technical analysis is overall lacking. This is particularly important for understanding the typological affinity between the pottery wares of Tianshanbeilu, those of the Yanbulak culture, and those of the Machang and Siba cultures. Does it denote the trade of pottery wares or population movement? Rice [9] used "stylistic analysis" to study the transfer of patterns of pottery wares among different groups of people, including intermarriage and technological learning. The knowledge of pottery styles (techniques and ideas) of group members (including potters), which have turned into fixed habits, is passed down from generation to generation; an excellent example is the pottery technology on the island of Mallorca, Spain, which lasted through much of the Bronze Age and into the Iron Age [10]. This thesis reveals the intrinsic motivation behind the spread of pottery wares, that is, the human-driven interactions. However, the "pottery style" itself is ambiguous and does not tell much about the diffusion mode of pottery wares. Is the similarity of pottery style the result of barter? Or the result of technological exchange or transfer of religious and artistic concepts? To answer these questions, the authors conducted a scientific analysis of the pottery wares of the Tianshanbeilu cemetery; for the sake of comparative analysis, they also conducted a scientific analysis of those excavated from the Yaer cemetery of the Yanbulak culture also in the Hami Basin, and cited the compositional data of the pottery wares excavated from the Xichengyi settlement of the Machang and Siba cultures in the Hexi corridor.

Samples and methods

In 2019, in cooperation with the Xinjiang Institute of Cultural Relics and Archaeology and the Hami Museum, the authors collected 70 samples from the Tianshanbeilu cemetery. In texture and color, these samples are comprised of seven types, i.e., coarse pottery in red, yellow, and gray, fine pottery in black and red (Fig. 10). In order to uncover the nature of the interaction of the Tianshanbeilu population within the Hami Basin and with the neighboring Hexi Corridor, the authors collected 26 samples of pottery samples from the Yaer cemetery of the Yanbulak culture in the Hami Basin, and the available compositional data of pottery samples excavated from the Xichengyi settlement of the Machang (2135-1880BC) and Siba (1880-1530BC) cultures near the city of Zhangye [11].

The compositional analysis of the abovementioned samples was carried out at the Laboratory of Conservation and Archaeometry of Ningbo Museum with an Oxford X-Met 8000 energy dispersive X-ray fluorescence (ED-XRF) spectrometer. The areas to be tested are newly cut sections, black paint, and red slip on the surface. The reference material is Getty Center ceramic from MBH (MBH Analytical Ltd), U.K. The major, minor, and trace elements of the samples were analyzed with voltages of 25 kV and 50 kV, currents of 600 μA and 300 μA, respectively, and test times of 60 s.

Petrographic analysis, a fundamental method for the study of technique and provenance of pottery [12–15], was undertaken at Nanjing Hongchuang Geological Company with the SD-3000A automatic optical scanning system coupled with Abbe NA 0.9 spotting scope made by MAITEWEI. The authors made 0.03 mm optical thin sections of selected samples to identify the clay matrix, types of detrital particles (tempers), and pores in the bodies. The mineralogical analysis was performed on a TTR-III X-ray diffractometer from Rigaku, Japan, at the Physical and Chemical Experiment Center of the University of Science and Technology of China, with an operating wavelength of Cu kα line ($\lambda = 1.54178$ Å), an operating voltage of 40 kV, an operating current of 200 ma, a scanning step of 0.02 degree, a scanning speed of 8 deg/min, and a scanning range of 10–70 degrees.

Raman spectroscopy is widely used in the identification of ceramic pigments [16–18]. To study the black and red pigments on the painted pottery from the Tianshanbeilu cemetery, the authors used a Witec laser confocal micro-Raman system (Alpha 300R) operated with an excitation wavelength of 532 nm, a grating of 600 g/mm, BLW (blue laser wavelength) = 500 nm, a lens of Zeiss EC Epiplan-Neofluar100, a laser output power of 15 MW, an integration time of 1 s, and a cycle number of 10.

Results

Sources of raw materials

Compositional data of the bodies

The authors eliminated the elements with significant overall errors or below detection limits and selected a total of 13 major (over 2%), minor (0.1–2%), and trace (< 0.1%) elements with relatively stable levels, namely Al, Si, K, Ca, Ti, Mn, Fe, Zn, Cu, Rb, Sr, Zr and Ba, all expressed as oxides. In the bodies of ancient ceramics, the most abundant oxide is SiO_2, followed by Al_2O_3,

which forms the skeleton of them. Some oxides R_xO_y (K_2O, CaO, Fe_2O_3, TiO_2, MnO), which have comparatively stronger fluxing effects, are usually added as tempers in coarse pottery to improve the sintering of the bodies.

The compositional data (Table 1) show that the SiO_2 amounts of the unpainted red coarse pottery samples range from 51.67 to 57.57%, and the Al_2O_3 amounts range from 18.62 to 21.32%; the SiO_2 and Al_2O_3 amounts of the painted red coarse pottery samples are not much different; only the SiO_2 amount of Sample 15 drops to 45.68%.In Fig. 2a, it is easy to see that the Al_2O_3 amounts of black fine pottery are significantly higher than those of the other types of pottery. Except for Sample 49, which has a low Al_2O_3 amount of 20.52%, the average Al_2O_3 amounts of the other samples reach 23.28%, indicating that the black fine pottery is made of clay with a high aluminum content.

From Fig. 3, One can see that the average SiO_2/Al_2O_3 ratio is relatively more stable for the red and black fine pottery and unpainted gray coarse pottery samples, which may be explained by the fact that these samples have fewer impurities in the bodies, but finer pastes, a speculation supported by the petrographic observations given below.

The oxide amounts of the various fluxes also reflect the compositional characteristics of the raw materials for the seven types of samples. In Fig. 2b, the CaO amounts of these types are approximately less than 3%; only Samples 59 and 66 of the red fine pottery have significantly higher CaO amounts; the K_2O amounts of the coarse pottery types and black fine pottery range from 1.25% to 3%. Among the red fine pottery samples, the K_2O amounts are lower (0.92–1.36%), except for Sample 66, which has outstandingly high Ca and K amounts; in Fig. 2c, the Fe_2O_3 amounts of the coarse pottery types are mostly located within the range of 4–8%, and the TiO_2 amounts within the range of 0.35–0.65%; the Fe_2O_3 amounts of the black fine pottery samples are mostly located within the range of 3.5–6.5%, comparable with those of the coarse pottery types, but the TiO_2 amounts are higher (above 0.5%). In contrast, the TiO_2 amounts of the red fine pottery samples are generally low, different from those of the black fine pottery ones.

In Fig. 2d, the amounts of Rb_2O and ZrO_2 are higher in the black fine pottery than those in the other pottery types, further reflecting the differences in their chemical compositions. Among them, the amounts of Rb_2O and ZrO_2 of the red and black fine pottery samples are widely separate, whereas those of the other five types are located between them. Since trace elements are not affected by the washing and firing processes, they sensitively illustrate the compositional differences of the seven sample types and effectively supplement the major and minor elements [19].

To further extrapolate the compositional characteristics of the samples from the Tianshanbeilu cemetery, the authors submitted the oxides other than MnO (low significance) to principal component analysis (PCA). PCA is a data transformation technique that exploits the correlation among the data variables in order to construct a new set of variables [20]. In Fig. 4, the aggregation of unpainted and painted red coarse pottery samples is rather apparent, reflecting the homogeneity of the compositions of the two types of pottery; the difference between them lies merely in the application of paint or not; the yellow (unpainted and painted) and gray coarse pottery samples fall within the same cluster, indicating that the raw materials for these types are similar. The red and black fine pottery samples are set widely apart. The data points of the red fine pottery samples are clustered in one area, with the exception of Sample 66; the black fine pottery samples are concentrated in a separate aggregation area, only overlapping slightly with those of the coarse pottery samples, with a relatively higher degree of dispersion.

Petrographic analysis

Based on the results of compositional analysis, the authors selected six pieces, including one painted red coarse, two unpainted yellow coarse, one painted yellow coarse, one painted red, and one unpainted black fine, from the above types of samples for petrographic analysis. The petrographic phase of a pottery sample is usually comprised of clay matrix, detrital particles, and pores; the clay matrix is comprised of clay particles (< 0.002 mm) [21], fine grit particles, and silt (0.002 mm–0.05 mm) [22]; the diameters of the detrital particles, which are generally larger than 0.05 mm, can be further divided into two categories: artificially added temper and natural inclusion. Most detrital particles of the coarse pottery types are artificially added tempers and are characterized by low roundness, mostly sub-angular shapes, and good sorting conditions [23]. One can assume that ancient potters intentionally crushed rock and sifted particles before mixing them into clay.

The proportions of tempers in the bodies of the coarse pottery types are mostly between 25 and 35%, indicating that the formulae are relatively homogeneous. The major types of tempers are silica-aluminate mineral particles such as quartz, plagioclase, striated feldspar, and granite fragments (Fig. 5), followed by pyroxene (ferrite–magnesium minerals), sericite, gneiss (metamorphic rock), sandstone, and a small amount of organic matter. Sericite, found mainly in shallow metamorphic rocks, can reduce the firing temperature of pottery and improve

Table 1 Compositional data of the Tianshanbeilu pottery samples

Typles	Tomb No	Sample No	Al_2O_3%	SiO_2%	K_2O%	CaO%	TiO_2%	MnO%	Fe_2O_3%	CuO ppm	ZnO ppm	Rb_2O ppm	SrO ppm	ZrO_2 ppm	BaO_2 ppm	SiO_2/Al_2O_3
Unpainted red coarse pottery	M9	1	20.71	53.39	1.80	1.76	0.44	0.12	5.53	28	55	108	216	132	458	2.58
	M7	2	21.32	51.67	2.34	2.93	0.57	0.13	6.98	40	76	153	291	182	590	2.42
	M9	3	21.07	55.13	1.58	2.04	0.37	0.12	5.37	25	55	97	209	124	493	2.62
	/	4	19.92	53.39	1.30	1.16	0.35	0.10	4.69	21	52	75	254	101	637	2.68
	M51 (III)	5	18.62	54.62	1.57	0.82	0.48	0.12	5.34	24	61	99	207	130	491	2.93
	/	6	20.59	56.83	2.17	0.90	0.55	0.09	6.06	23	75	114	128	152	465	2.76
	M354 (III)	7	20.68	57.57	1.93	0.81	0.52	0.13	4.95	20	62	94	135	104	367	2.78
	M13 (III)	8	20.20	56.41	1.75	0.99	0.55	0.07	5.29	22	63	99	295	160	543	2.79
	Average		20.39	54.88	1.80	1.43	0.48	0.11	5.53	25.38	62.38	104.88	216.88	135.63	505.5	2.70
	Stdev		0.79	1.88	0.32	0.71	0.08	0.02	0.66	6	8.4	21.07	58.88	25.96	78.49	0.15
Painted red coarse pottery	T8R9	9	18.82	56.12	1.29	1.27	0.37	0.16	4.16	19	42	71	145	105	397	2.98
	M519	10	20.71	54.01	1.87	1.52	0.43	0.06	5.15	23	58	84	173	110	387	2.61
	M530	11	19.74	54.76	1.76	1.73	0.40	0.09	4.97	19	55	82	376	98	419	2.77
	M354 (III)	12	20.56	51.53	1.96	1.56	0.54	0.08	6.96	31	67	109	479	167	658	2.51
	M437	13	21.83	53.70	2.43	3.07	0.61	0.12	7.85	39	101	204	361	170	861	2.46
	M518 (II)	14	20.12	54.27	2.06	2.12	0.49	0.07	5.93	32	65	113	185	136	530	2.70
	/	15	20.84	45.68	1.75	1.76	0.51	0.35	8.01	26	71	112	182	130	421	2.19
	M201	16	20.22	53.40	1.97	1.78	0.58	0.18	7.45	43	100	145	319	195	563	2.64
	M631	17	20.84	54.89	2.09	0.86	0.55	0.12	5.72	29	73	119	169	144	464	2.63
	/	18	18.69	55.32	1.25	0.62	0.39	0.16	4.70	19	50	79	133	115	347	2.96
	T8R9	19	19.65	56.64	1.71	1.66	0.47	0.12	5.69	29	65	112	177	131	453	2.88
	M294	20	20.74	56.09	2.37	1.34	0.63	0.10	6.78	28	82	167	281	210	533	2.70
	M631	21	21.25	52.63	1.93	0.82	0.52	0.11	5.13	25	63	97	151	114	370	2.48
	M201	22	21.17	54.49	2.41	1.95	0.69	0.13	8.44	34	105	163	305	202	604	2.57
	M47 (III)	23	21.64	50.34	1.75	1.35	0.55	0.10	5.42	27	63	93	165	117	355	2.33
	M1 (II)	24	19.51	53.58	1.33	0.90	0.35	0.08	4.60	19	55	92	172	104	1715	2.75
	Average		20.40	53.59	1.87	1.52	0.51	0.13	6.06	27.63	69.69	115.13	235.81	140.5	567.31	2.64
	Stdev		0.90	2.60	0.36	0.58	0.10	0.07	1.3	6.94	17.98	35.81	100.20	35.9	323.73	0.21

Table 1 (continued)

Types	Tomb No	Sample No	Al_2O_3%	SiO_2%	K_2O%	CaO%	TiO_2%	MnO%	Fe_2O_3%	CuO ppm	ZnO ppm	Rb_2O ppm	SrO ppm	ZrO_2 ppm	BaO_2 ppm	SiO_2/Al_2O_3
Unpainted yellow coarse pottery	M355	25	21.51	50.31	1.83	0.77	0.62	0.17	6.01	39	67	104	218	154	486	2.34
	/	26	20.68	57.48	2.10	1.23	0.64	0.10	5.82	29	73	107	225	186	596	2.78
	M626 (I)	27	20.00	52.98	2.75	1.02	0.69	0.16	7.62	48	93	144	216	156	488	2.65
	M700	28	21.33	49.93	2.24	1.52	0.64	0.14	7.27	38	108	135	446	169	617	2.34
	M170	29	22.81	52.48	2.00	1.99	0.52	0.09	6.09	35	70	116	195	164	514	2.30
	M5 (III)	30	20.95	47.89	1.79	2.69	0.53	0.10	7.01	35	79	114	183	136	650	2.29
	M19 (IV)	31	21.01	53.05	2.29	1.49	0.64	0.08	7.14	36	99	134	386	173	667	2.53
	/	32	22.03	51.93	2.67	1.05	0.59	0.20	6.43	24	82	175	226	169	644	2.36
	/	33	20.40	58.58	2.67	1.92	0.69	0.11	7.06	29	85	166	335	197	781	2.87
	/	34	19.86	56.98	1.90	1.14	0.61	0.12	6.46	28	80	122	264	178	601	2.87
	/	35	20.12	58.91	2.10	0.94	0.60	0.10	5.47	30	66	103	207	192	516	2.93
	Average		20.97	53.68	2.21	1.43	0.62	0.12	6.58	33.73	82	129.09	263.73	170.36	596.36	2.57
	Stdev		0.87	3.58	0.33	0.54	0.05	0.04	0.65	6.35	12.84	23.35	82.57	17.02	86.25	0.25
Painted yellow coarse pottery	M692 (II)	36	20.47	55.35	1.62	2.17	0.46	0.07	5.32	25	58	102	206	141	497	2.70
	/	37	20.21	59.10	2.06	2.12	0.51	0.14	5.26	22	66	120	169	139	1864	2.92
	Average		20.34	57.22	1.84	2.14	0.49	0.11	5.29	23.5	62	111	187.5	140	1180.5	2.81
	Stdev		0.13	1.87	0.22	0.02	0.02	0.03	0.03	1.5	4	9	18.5	1	683.5	0.11

Table 1 (continued)

Types	Tomb No	Sample No	Al_2O_3%	SiO_2%	K_2O%	CaO%	TiO_2%	MnO%	Fe_2O_3%	CuO ppm	ZnO ppm	Rb_2O ppm	SrO ppm	ZrO_2 ppm	BaO_2 ppm	SiO_2/Al_2O_3
Unpainted black fine pottery	T18	38	22.30	55.82	1.55	1.11	0.55	0.07	4.30	71	72	115	300	248	594	2.50
	M700	39	24.51	53.20	2.53	2.51	0.79	0.08	6.63	38	76	216	732	273	909	2.17
	/	40	24.49	58.14	2.18	0.79	0.74	0.07	4.00	28	62	137	175	172	441	2.37
	/	41	21.86	52.85	2.74	2.47	0.65	0.19	7.07	32	96	142	354	133	635	2.42
	/	42	23.99	58.84	2.15	0.96	0.65	0.03	2.76	40	44	100	310	139	342	2.45
	M301 (II)	43	23.13	57.29	2.53	2.19	0.67	0.14	5.69	31	73	164	330	257	789	2.48
	M144 (III)	44	22.40	54.52	2.28	1.34	0.64	0.12	6.23	16	88	149	228	201	692	2.43
	/	45	23.35	54.69	2.72	1.97	0.70	0.15	6.00	31	75	168	349	270	899	2.34
	M522	46	22.45	52.99	2.47	1.33	0.63	0.12	6.88	26	87	140	564	181	871	2.36
	M479	47	22.01	51.93	2.94	1.08	0.73	0.18	7.92	40	117	197	250	193	658	2.36
	/	48	24.96	50.96	2.00	2.06	0.63	0.21	5.42	54	74	163	681	363	733	2.04
	/	49	20.52	56.75	1.72	1.63	0.44	0.06	4.96	20	60	91	312	109	514	2.77
	/	50	25.12	50.36	2.26	0.76	0.59	0.05	4.53	34	46	147	168	245	576	2.00
	M294	51	23.32	58.24	1.88	2.48	0.66	0.11	4.90	35	48	121	519	269	576	2.50
	M210 (III)	52	22.22	55.45	1.94	1.37	0.66	0.10	5.85	21	56	142	360	258	793	2.50
	T21	53	23.49	55.99	2.54	1.12	0.62	0.20	5.54	24	75	137	271	228	906	2.38
	/	54	22.68	54.57	2.30	1.15	0.54	0.07	4.93	27	58	170	270	243	607	2.41
	/	55	23.37	55.46	2.77	1.15	0.71	0.22	6.06	29	89	138	357	244	934	2.37
	/	56	22.96	54.67	2.00	1.16	0.67	0.13	4.45	66	73	119	253	286	655	2.38
	M664	57	23.67	56.13	2.23	2.73	0.76	0.13	6.11	84	137	148	506	296	632	2.37
	M587	58	23.28	50.49	1.75	1.85	0.56	0.08	5.44	27	59	103	349	184	726	2.17
	Average		23.15	54.73	2.26	1.62	0.65	0.12	5.50	36.86	74.52	143.19	363.71	228.19	689.62	2.37
	Stdev		1.09	2.44	0.37	0.58	0.08	0.05	1.15	17.24	22.26	29.78	149.13	59.74	157.2	0.16

Table 1 (continued)

Types	Tomb No	Sample No	Al_2O_3%	SiO_2%	K_2O%	CaO%	TiO_2%	MnO%	Fe_2O_3%	CuO ppm	ZnO ppm	Rb_2O ppm	SrO ppm	ZrO_2 ppm	BaO_2 ppm	SiO_2/Al_2O_3
Painted red fine pottery	M17 (III)	59	21.99	55.66	1.36	4.45	0.44	0.10	5.19	36	68	67	274	85	456	2.53
	/	60	20.83	44.40	0.94	1.58	0.52	0.11	6.75	38	60	70	145	79	257	2.13
	/	61	20.28	54.79	0.92	1.83	0.22	0.07	2.88	13	25	41	149	38	236	2.70
	M521	62	20.77	46.81	0.92	3.45	0.33	0.65	6.27	24	67	47	225	78	392	2.25
	M317 (II)	63	21.96	53.92	1.12	1.96	0.34	0.07	3.62	18	34	54	160	54	232	2.46
	/	64	21.17	53.80	1.45	2.23	0.38	0.09	4.28	24	48	82	179	89	307	2.54
	T1018	65	20.08	49.12	1.04	2.00	0.26	0.21	4.59	15	40	51	106	49	276	2.45
	T1018	66	22.88	50.63	2.58	5.72	0.72	0.21	9.10	45	107	191	346	151	718	2.21
	Average		21.25	51.14	1.29	2.90	0.40	0.19	5.33	26.63	56.13	75.38	198	77.88	359.25	2.41
	Stdev		0.90	3.83	0.52	1.40	0.15	0.18	1.86	10.98	24.1	45.48	74.07	32.63	154.37	0.18
Unpainted gray coarse pottery	M682 (IV)	67	21.09	49.67	2.11	1.15	0.59	0.10	6.89	37	83	135	403	168	558	2.35
	M311 (II)	68	20.28	47.58	1.87	0.84	0.48	0.10	6.23	30	74	115	368	193	664	2.35
	/	69	20.73	54.28	1.76	2.73	0.49	0.07	5.26	30	63	97	242	146	576	2.62
	/	70	21.51	53.36	2.03	3.85	0.58	0.08	6.13	20	73	113	291	179	601	2.48
	Average		20.90	51.22	1.94	2.14	0.53	0.09	6.13	29.25	73.25	115	326	171.5	599.75	2.45
	Stdev		0.45	2.72	0.14	1.22	0.05	0.01	0.58	6.06	7.08	13.49	63.19	17.18	40.11	0.11

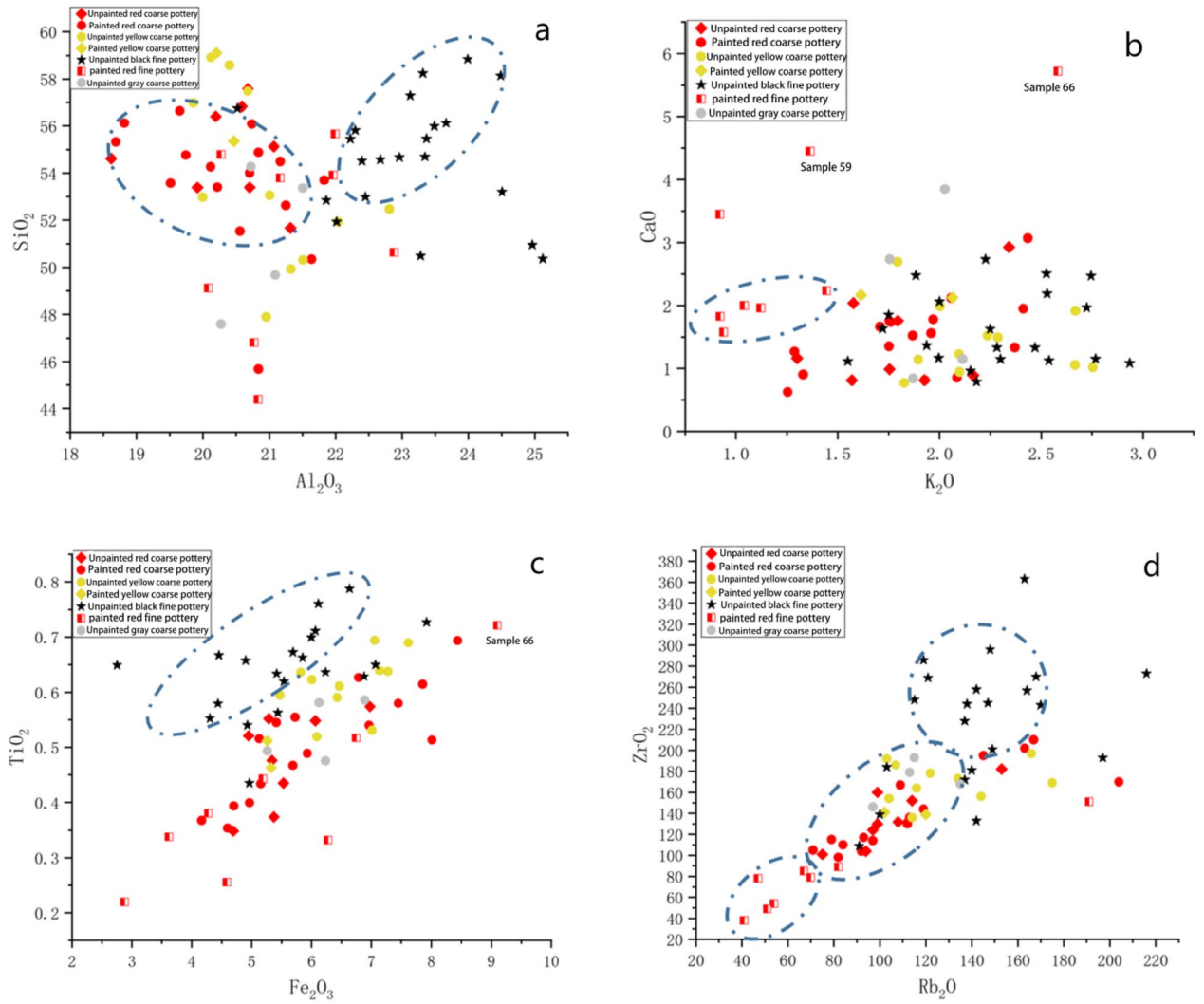

Fig. 2 Binary scatter diagram of index oxides

the strength of the body; it is mainly used in low- and medium-temperature kilns. The red or yellowish-brown colors of the coarse pottery samples under the microscope indicate the precipitation of iron (Fig. 5a–d); the mineral tempers such as sericite, quartz, and feldspar may denote that the potters had not yet mastered high-temperature firing. This observation agrees well with the higher contents of fluxes in the compositional analysis.

The red and black fine pottery samples have relatively fewer detrital particles than the coarse pottery ones. The clay matrix, which makes up 70% to 90% of the body, is comprised primarily of fine silt and clay particles and is weakly translucent under polarized light microscopy, all of which indicate that the clay of these samples is finely washed. The microscopically visible detrital particles may have been the natural components of the soil; black organic debris and irregular pores are visible in the bodies of the black fine pottery samples (Fig. 5e, f). In addition, it is worth mentioning that Sample 66 contains limestone particles, which are derived from the carbonate rock group (Fig. 5e), a typical sedimentary rock [24]. One may assume that the painted red fine pottery sample is made of clay from a separate source of sedimentary clay near a river or a lake. The images of X-ray diffraction (Fig. 6) show that the mineralogical compositions of the six samples are mainly comprised of quartz, feldspar, illite, alumina, zeolite, white mica (including sericite), and hematite, which is generally consistent with the observation that the silica-aluminate mineral detrital particles are predominant in the petrographic images (Fig. 5). Among them, the (unpainted and painted) red

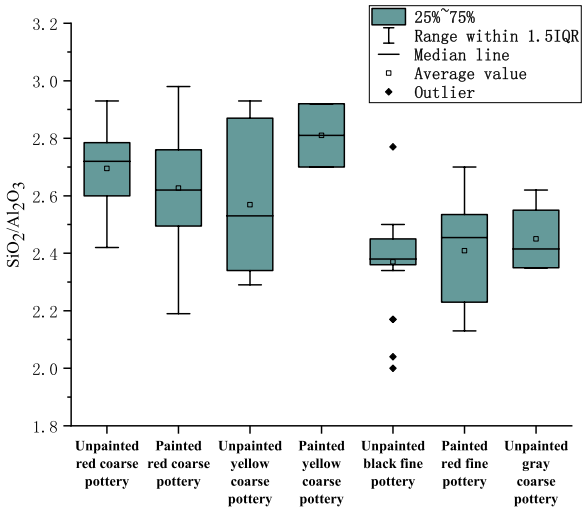

Fig. 3 Box line diagram of SiO_2 and Al_2O_3 molar ratios

and unpainted yellow coarse pottery unambiguously contains hematite (Fig. 6a–c), again consistent with the high amounts of ferrite oxide (Fig. 2c) and petrographic images.

(Fig. 5a–c).

With the ED-XRF, petrographic, and mineralogical analyses, the authors explored into the compositional and technical characteristics of the seven types of samples, especially the coarse pottery and fine pottery ones, from the Tianshanbeilu cemetery. In their studies of the compositional characteristics of pottery samples from the Neolithic Dadiwan site (5800-2800BC) in Qin'an County, Gansu Province, in the western part of the Loess Plateau, Qinglin Ma et al. [25] and Hongjiao Ma et al. [26] identified two types of pottery wares, one made of local red clay and the other probably brought from outside by immigrating people or through exchange. This thesis is applicable to the pottery samples from the Tianshanbeilu cemetery. The above analytical data show that the coarse pottery samples in red, yellow, and gray are compositionally similar, implying that they were produced out of clay from one source. The chemical compositions of the red and black

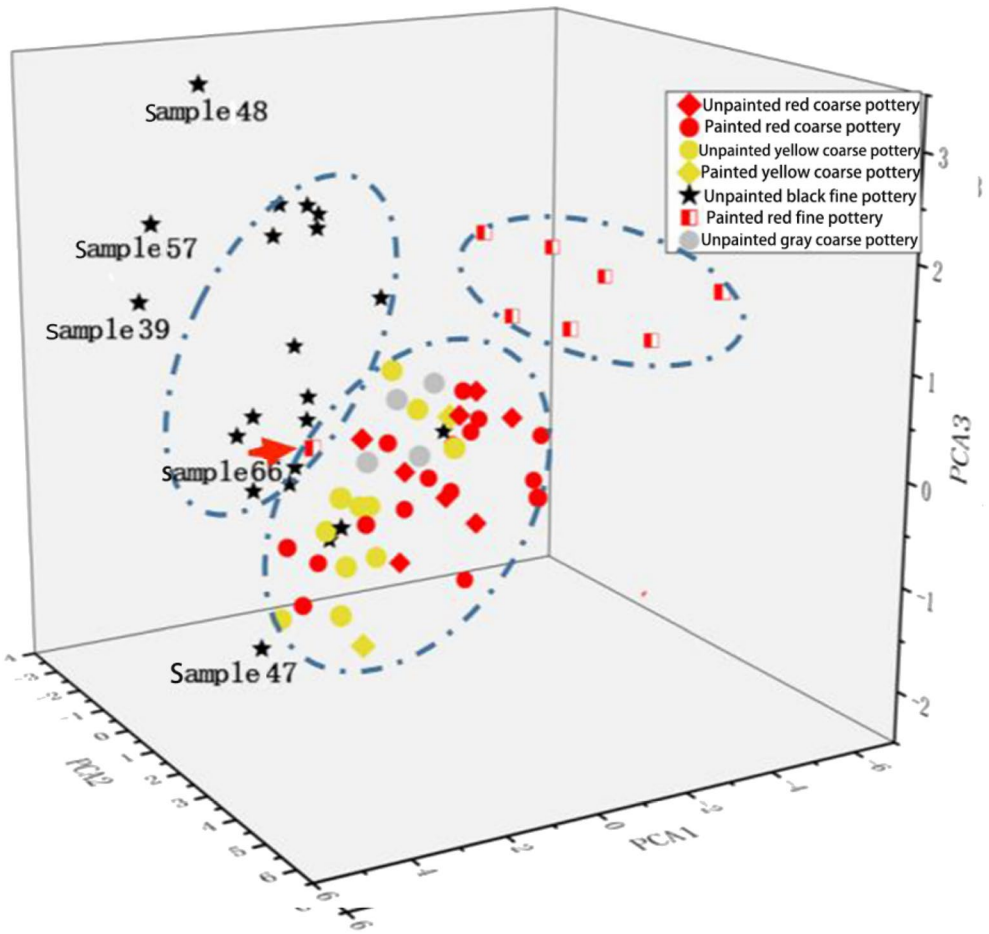

Fig. 4 Diagram of principal component analysis

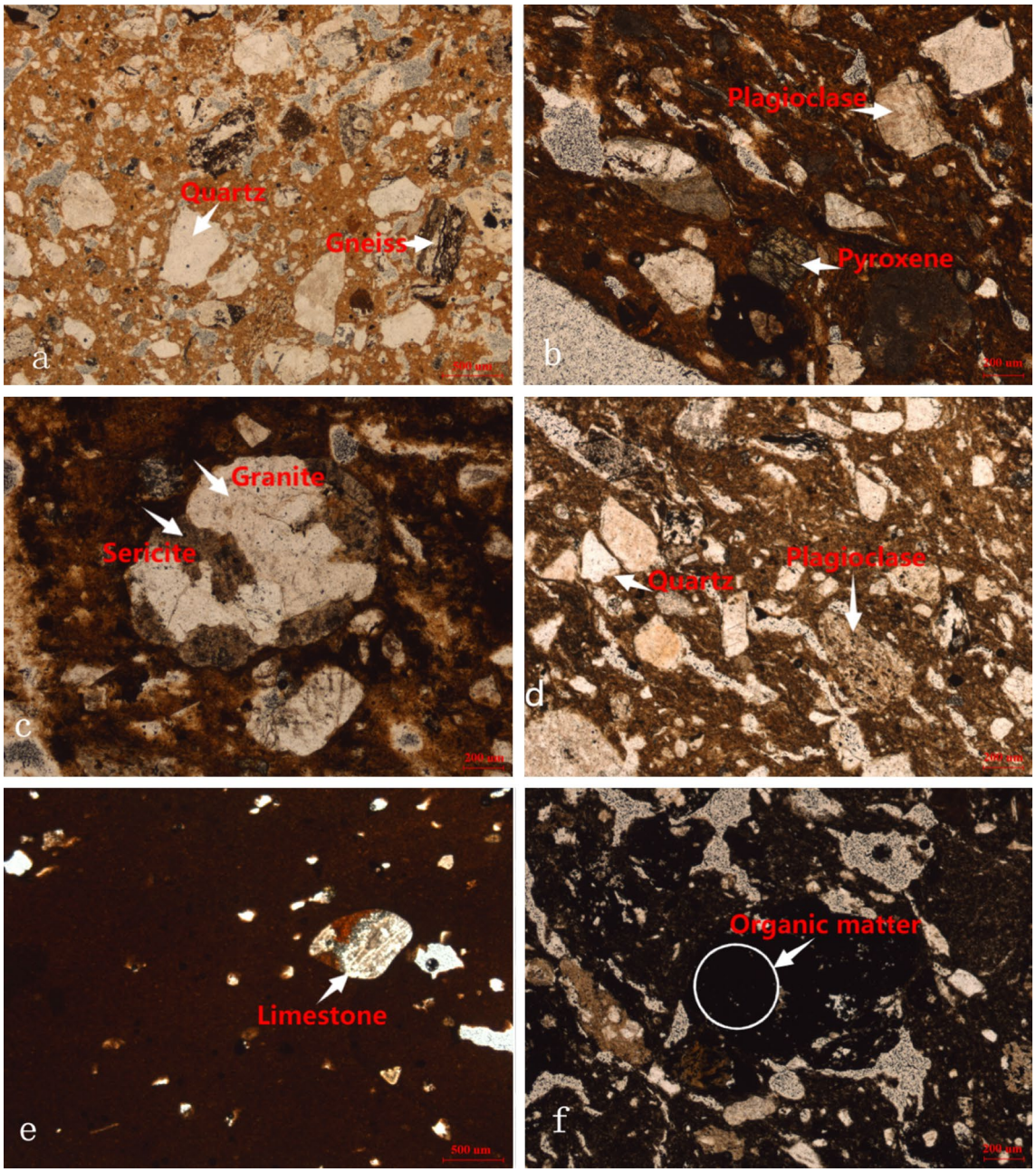

Fig. 5 Petrographic images of the six samples. **a** Sample 12 (painted red coarse pottery); **b** Sample 28 (unpainted yellow coarse pottery); **c** Sample 27 (unpainted yellow coarse pottery); **d** Sample 37 (painted yellow coarse pottery); **e** Sample 66 (painted red fine pottery); **f** Sample 44 (unpainted black fine pottery). The photos are taken under single polarized light

fine pottery samples are very different from those of the coarse pottery, suggesting separate sources of clay for the production of these samples. At present, no contemporary kiln has been discovered in the Hami Basin, and no clay sample has been analyzed; it is difficult to pinpoint the provenance of the two groups of samples.

Coloring and carburizing techniques

The painted pottery wares from the Tianshanbeilu cemetery are quite distinctive, featuring motifs of triangles, vertical stripes, waves, and diamond lattices. The paint is mostly black; under the black paint, most of the red coarse pottery has a red slip. The authors selected six samples and compared the amounts of the major and

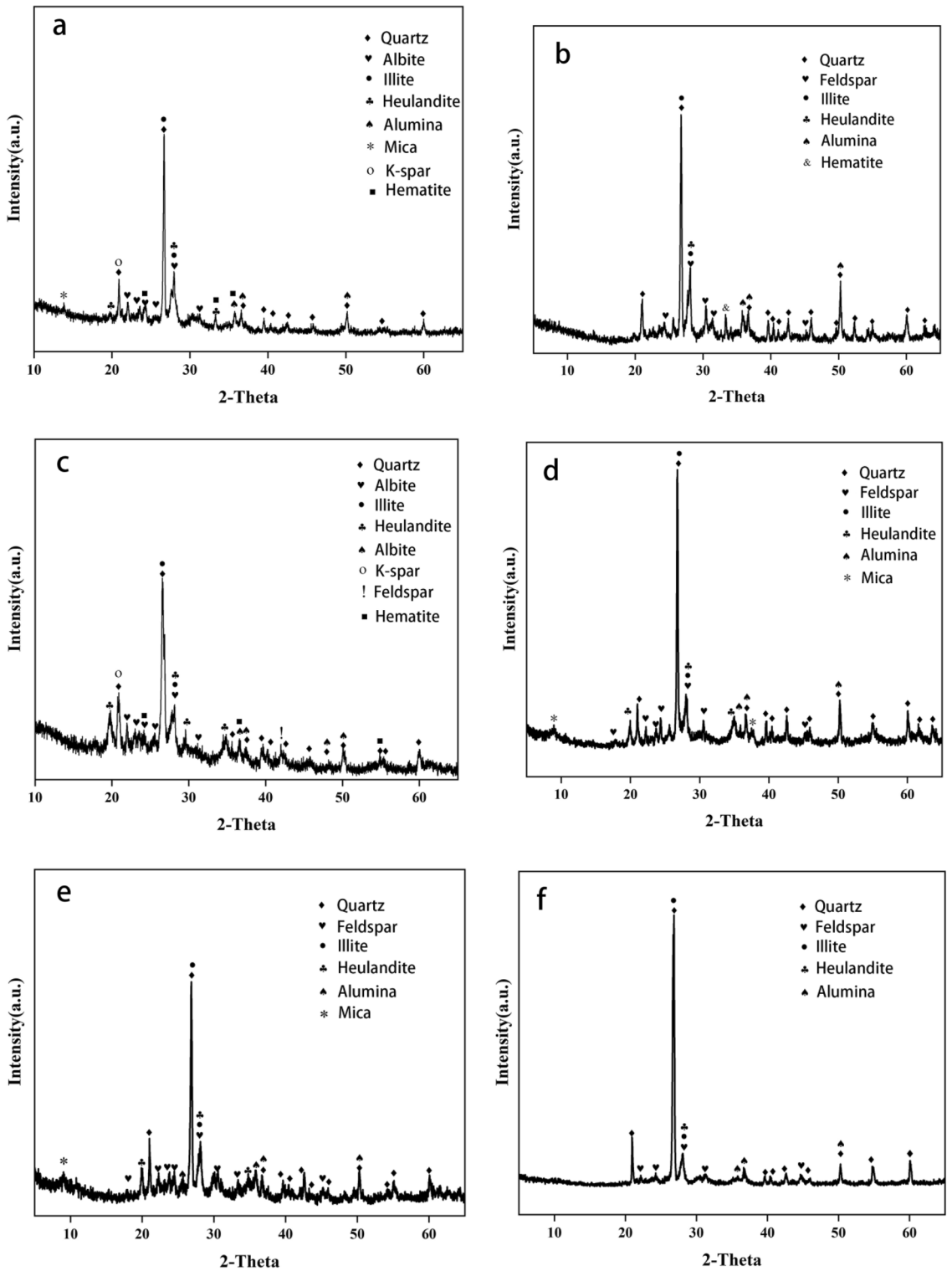

Fig. 6 Mineralogical analysis of the six samples. **a** Sample 7 (unpainted red coarse pottery); **b** Sample 17(painted red coarse pottery); **c** Sample 28 (unpainted yellow coarse pottery); **d** Sample 68 (unpainted gray coarse pottery); **e** Sample 65 (painted red fine pottery); **f** Sample 57 (unpainted black fine pottery)

minor oxides of the black paints, red slips, and red bodies (Table 2). In addition, they analyzed the surfaces of Sample 12, which features red slip and black paint, and Sample 36, which features black paint, with Raman spectroscopy to compare them and explore the coloring mechanism of black paint and red slip.

As seen in Table 2 and Fig. 7, the Fe_2O_3 amounts of the black paints and red slips range from 8.59 to 16.35%, whereas those of the corresponding red bodies are significantly lower, ranging from 4.16 to 6.98%; the MnO amounts of both the black paints and red slips are higher than those of the red bodies. In comparison, the MnO amounts of the black paints are rather high, up to 5.83%, whereas those of the red slips range from 0.19 to 0.25%. Raman spectrometry shows that the red slip of Sample 12 has peaks at wavenumber 279 cm^{-1} and 504 cm^{-1} (Fig. 8a), similar to the characteristic peaks of hematite at 290 cm^{-1}, 505 cm^{-1}, and 613 cm^{-1} [27–29], indicating

Table 2 Compositional data of the red slips, black paints, and red bodies of the six samples wt% (partial)

Sample No	Pottery types	Tested areas	Al_2O_3%	SiO_2%	K_2O%	CaO%	TiO_2%	MnO%	Fe_2O_3%
2	a	Red slip	21.67	52.95	2.51	4.15	0.66	0.19	8.59
		Red body	21.32	51.67	2.34	2.93	0.57	0.13	6.98
3	a	Red slip	18.46	44.80	2.48	1.46	0.67	0.25	13.19
		Red body	21.07	55.13	1.58	2.04	0.37	0.12	5.37
9	b	Black paint	17.50	53.79	2.18	3.73	0.73	1.09	9.33
		Red body	18.82	56.12	1.29	1.27	0.37	0.16	4.16
12	b	Black paint	14.40	44.51	1.93	2.03	0.64	5.83	9.92
		Red body	20.56	51.53	1.96	1.56	0.54	0.08	6.96
18	b	Black paint	17.77	50.64	1.81	2.35	0.67	1.04	9.96
		Red body	18.69	55.32	1.25	0.62	0.39	0.16	4.70
65	c	Black paint	11.48	45.00	1.28	3.38	0.43	1.26	16.35
		Red body	20.08	49.12	1.04	2.00	0.26	0.21	4.59

a. Unpainted red coarse pottery; b. Painted red coarse pottery; c. Painted red fine pottery

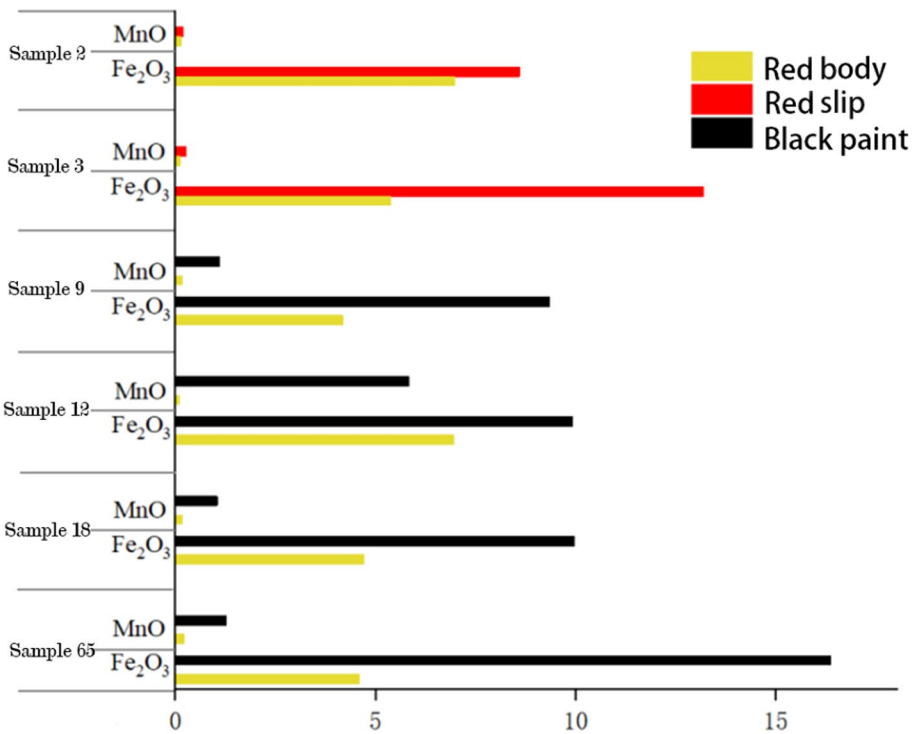

Fig. 7 MnO and Fe_2O_3 contents of red slip, black paints, and red bodies of the six samples

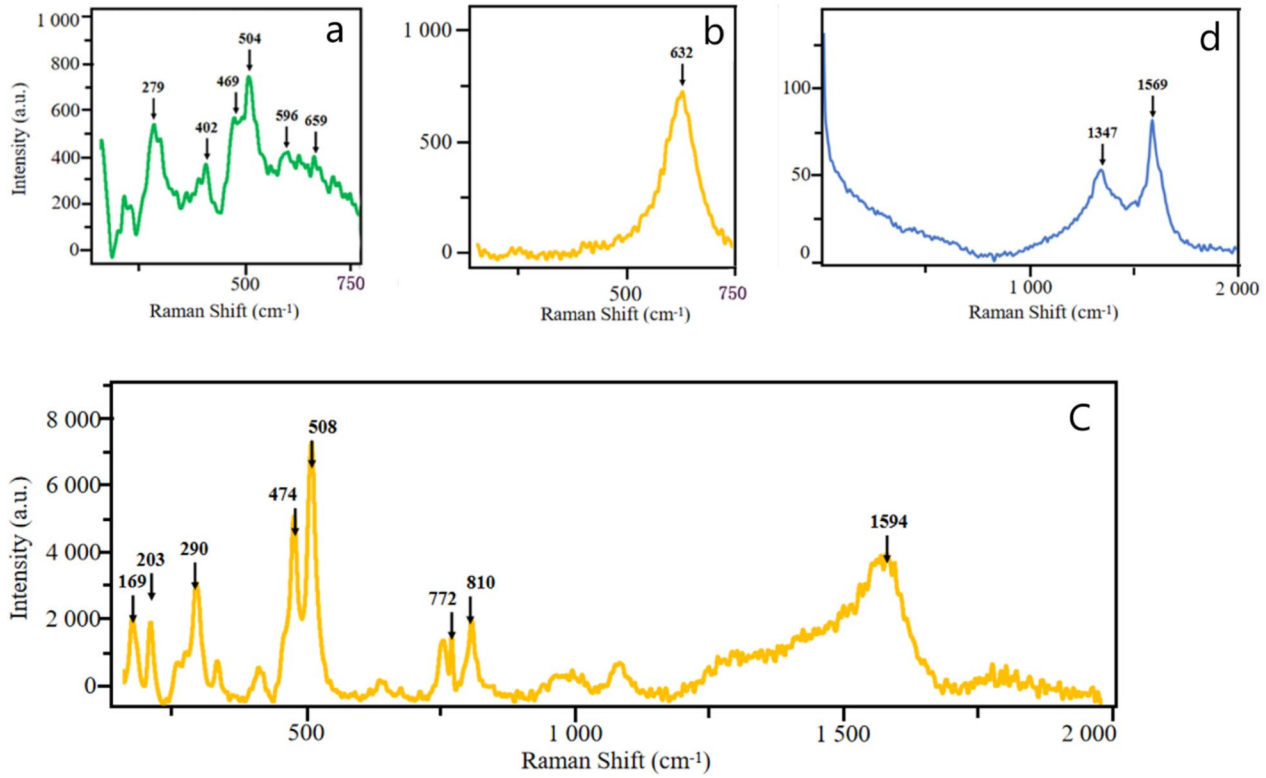

Fig. 8 Raman analysis of the surfaces of pottery samples (**a**, **b** Sample 12; **c** Sample 36; **d** Sample 67)

that its mineral phase is hematite (α-Fe_2O_3). The Raman shifts may have been due to the small grain size [30]. The black paint of Sample 12 has peaks at 632 cm^{-1} (Fig. 8b), which corresponds to the characteristic peak of Mn_3O_4 (black manganese) [31, 32]. For the black paint of Sample 36, the Raman spectroscopy does not show a peak in the range of black manganese, but there is a strong peak at 1594 cm^{-1} (Fig. 8c), almost identical with the standard peak of carbon black (1595 cm^{-1} and 1597 cm^{-1}) [33, 34], indicating that the raw material for the black paint of this sample is carbon black.

Chen et al. [35] found that the black paints of the Majiayao pottery are made of zinc-iron spinel, magnetite, and black manganese ore. Li [36] found that those of the painted pottery from the Guanmiaoshan site in Zhijiang, Hubei province, are made of local iron-manganese nodules. The iron and manganese deposits are quite rich in the Hami Basin. The iron ore reserves of this region rank first in Xinjiang, and the manganese ore deposit is shallow and easily accessible.

In addition to a large amount of painted pottery, the Tianshanbeilu cemetery yielded gray coarse pottery and black fine pottery, the former characterized by the polished gray-black surface, and the latter characterized by a "black body in cross-section, light yellow and light red on surfaces." It has been shown that the carburizing technique, infusing thick smoke into a closed kiln during firing and infiltrating carbon particles onto the surfaces of pottery wares, was involved in the production of gray coarse pottery. Sample 67 shows strong peaks at 1347 m^{-1} and 1569 m^{-1} (Fig. 8d), again close to the characteristic Raman peak of carbon black.

From the above compositional analysis, one can see that the raw material for the coarse pottery in gray, red (unpainted and painted), and yellow (unpainted and painted) is almost the same. The gray coarse pottery is fired in a reducing kiln, and the carburizing technique is used during the firing; the surface is further polished to make the surface smoother and denser; the other types of coarse pottery are fired in oxidizing kilns; most of the red coarse pottery is coated with red slip and painted with black pigment. The black fine pottery is not only different in raw material but also in firing technique. The "black inside and red outside" pottery is distinctive and may have been fired first in reducing kilns but later exposed to air.

Patterns of interaction between Tianshanbeilu, Yaer, and Xichengyi

As stated earlier, the pottery wares from the Tianshanbeilu cemetery have been of great interest to the scholarly community because they are the key to the question of the origin of the Tianshanbeilu culture. In typology, the pottery wares are affiliated with those of the Machang and Siba cultures in the Hexi Corridor to the east. Li [4] has suggested that peoples of the Hexi Corridor migrated to eastern Xinjiang, giving rise to the Tianshanbeilu culture and subsequently contributing to the formation of the Yanbulak culture in the Hami Basin. Therefore, the authors used the compositional data to explore the relationship between the pottery wares from Tianshanbeilu, Xichengyi, a settlement of the Machang and Siba cultures in the Hexi Corridor, and Yaer, a cemetery of the Yanbulak culture in the Hami Basin, and the interaction between the people behind the production and exchange of the pottery wares.

The authors first analyzed the chemical composition of 26 pottery samples from the Yaer cemetery with ED-XRF (Table 3). They compared the data with those of the samples from Tianshanbeilu. The Yaer cemetery is located in the Baiyang River oasis, just over 60 km to the west of Tianshanbeilu, and dated to the late Bronze Age through the early Iron Age, roughly overlapping with the third and fourth phases of the Tianshanbeilu cemetery. In the diagram of principal component analysis (Fig. 9), one can see that some samples from the Yaer cemetery overlap with those of Tianshanbeilu. The majority, however, are concentrated in a separate area. In addition, the samples from Tianshanbeilu are more dispersed than the Yaer ones. One may infer from the facts that the populations of the two cemeteries exchanged some of the pottery wares or exploited the same source of clay for separate production. The Yaer samples are more consistent, mostly coated with red slip and painted in black, and decorated with wave patterns and short vertical stripes (Fig. 10). Similar patterns are found in the coarse pottery samples from the Tianshanbeilu cemetery.

The authors collected the composition data of pottery samples from the Xichengyi site (Table 3) and normalized them. At Xichengyi, pottery wares of the Machang and Siba cultures, dated to 2135-1530 BC, have been discovered. In Fig. 9, the data points are removed from those of the Tianshanbeilu and Yaer samples, forming an independent aggregation area, indicating that the pottery wares from the two sites are not of the same provenance. This phenomenon seems to contradict the existing observation that the painted pottery wares from Tianshanbeilu are typologically akin to those of the Machang and Siba cultures in terms of vessel shape, decoration, and color. This contrast, however, is not surprising at all because, as Hung et al. [37] pointed out, the exchange of pottery wares could occur through three different channels: migration of people, transfer of technology, and direct import of pottery; spread of technology usually accompanies migration of people. In a similar vein, Zhang et al. [38] found that the metal artifacts of Tianshanbeilu are typologically, morphologically, and technologically comparable with, yet in the meantime distinct from, those of the Siba culture and the Karasuk culture (1400-800BC) in the Minusinsk Basin, and argued that they were most likely produced locally with local sources of metal ores.

In terms of vessel shape and decoration, the pottery wares from the Tianshanbeilu cemetery (especially the double-ear jars) are reminiscent of the ones from the Xichengyi site (Fig. 10). However, they are not exactly the same. The double-ear jars from Tianshanbeilu have larger bellies; the lizard patterns painted on the ears of their counterparts of the Siba culture are absent on the jars of Tianshanbeilu. The double-ear cylindrical jars of Tianshanbeilu are not found among the pottery assemblage of the Siba culture. Therefore, the occurrence of pottery wares of the Machang and Siba cultures appears to have taken place as a result of technological transmission and cultural diffusion concurring with population migration. Although more analyses of pottery samples from the other sites of the cultures are required to establish the case, the present compositional and typological evidence favors the possibility that the Tianshanbeilu people used local clay to make pottery and modeled the major pottery wares on the prototypes of the Hexi Corridor (Fig. 11).

Conclusion

In the absence of more pertinent data, the results presented in this paper are somewhat premature. The compositional and petrographic data of 70 pottery samples from the Tianshanbeilu cemetery indicate that the red (unpainted and painted), yellow (unpainted and painted), and unpainted gray coarse pottery are similar in the principal component analysis; the raw materials for these types are procured from one source. In contrast, the red and black fine pottery types are sharply different in the above indexes, and their raw materials may have come from other sources. The provenance of the two groups of pottery samples, due to the lack of evidence from the contemporary kiln and the lack of analysis of local clay, cannot be pinned down at present.

In terms of pigments, the chromogenic phases of red and black paints on painted pottery are hematite and black manganese ore; carbon black is used as raw material for black paint; carburizing and polishing are used in the production of the unpainted gray coarse pottery. The black fine pottery differs from the other types of pottery

Table 3 Compositional data of the Yaer and Xichengyi pottery samples

Sample (yaer)	Al_2O_3%	SiO_2%	K_2O%	CaO%	TiO_2%	MnO%	Fe_2O_3%	Label(Xichengyi)	Al_2O_3%	SiO_2%	K_2O%	CaO%	TiO_2%	MnO%	Fe_2O_3%
HWYM93	18.17	52.40	1.81	4.02	0.50	0.11	5.16	1	17.91	58.66	3.85	4.84	0.5	0.09	8.55
HWYM1	19.20	53.96	1.48	3.89	0.43	0.10	5.42	2	16.79	61.48	3.41	5.42	0.53	0.11	7.57
HYWM440	21.21	54.21	2.23	4.58	0.53	0.19	6.22	3	17.05	60.05	3.42	4.24	0.54	0.14	8.48
HWYM227	19.21	55.55	2.28	4.89	0.51	0.22	6.13	4	17.2	62.37	4.43	2.38	0.81	0.08	7.87
HWYM174	18.65	54.59	2.11	4.79	0.53	0.14	5.89	5	17.26	59.7	3.66	4.6	0.6	0.18	8.59
HWYM206	17.90	55.56	1.84	2.99	0.53	0.10	5.06	6	18.34	59.58	3.87	4.17	0.52	0.1	8.14
HWYM440	19.21	55.49	2.22	5.30	0.51	0.18	5.86	7	14.69	59.5	2.56	5.98	0.78	0.13	9.84
HWYM174	19.84	56.65	1.85	3.02	0.48	0.11	5.32	8	16.47	62.32	3.29	3.93	0.52	0.14	7.69
HWYM206	19.22	55.98	1.74	4.15	0.45	0.08	4.67	9	16.98	61.98	3.75	3.4	0.64	0.09	8.3
HWYM416	21.29	57.74	1.91	3.13	0.43	0.11	4.71	10	18.28	58.02	4.09	5.02	0.54	0.13	8.36
HWYM314	19.90	57.18	2.01	4.66	0.50	0.10	5.09	11	16.15	61.61	2.25	2.99	0.73	0.12	10.33
HWYM431	17.91	57.07	1.13	2.23	0.40	0.06	3.82	12	16.05	60.81	2.59	4.87	0.6	0.13	9.47
HWYM388	20.87	56.77	1.13	3.40	0.36	0.10	4.04	13	16.85	60.66	3.66	4.08	0.67	0.14	8.89
HWYM302	20.51	59.38	1.96	3.51	0.42	0.08	4.67	14	16.62	60.15	4.25	3.14	0.7	0.11	9.44
HWYM4	20.88	58.51	1.93	4.54	0.50	0.09	4.86	15	16.19	59.82	3.23	5.02	0.58	0.13	9.14
HWYM227	21.08	57.57	2.15	4.81	0.53	0.10	5.36	16	17.19	57.39	3.47	5.31	0.67	0.13	9.73
HWYM159	20.29	57.04	2.32	6.04	0.57	0.14	6.21	17	15.19	59.36	2.9	6.12	0.61	0.13	8.81
HWYM275	19.67	58.50	2.11	5.53	0.49	0.10	4.77	18	15.45	59.82	2.99	5.76	0.68	0.11	8.98
HWYM426	20.34	59.61	2.31	5.42	0.50	0.17	5.35	19	17.06	57.97	3.41	5.51	0.66	0.12	8.97
HWYM284	20.80	55.43	2.29	5.94	0.70	0.14	6.94	20	16.73	60.52	3.67	4.42	0.65	0.11	8.56
HWYM374	19.98	53.60	2.57	4.72	0.76	0.12	6.49	21	18.77	58.98	4.13	4.75	0.56	0.09	8.03
HWYM440	21.27	56.22	2.75	6.27	0.63	0.13	7.44	22	18.93	57.88	4.33	3.12	0.56	0.07	8.93
HWYM202	20.07	57.42	1.98	5.00	0.43	0.09	4.86	23	15.8	59.5	2.49	4.5	0.74	0.12	10.79
HWYM388	21.38	53.69	1.44	4.89	0.53	0.14	6.11	24	16.25	57.99	2.9	5.1	0.65	0.13	10.17
HWYM159	19.35	54.90	2.30	4.36	0.60	0.09	5.90	25	17.23	58.96	4.38	4.47	0.63	0.11	8.91
HWYM318	19.98	58.33	1.94	6.69	0.52	0.09	5.64	26	16.69	57.57	2.97	5.82	0.66	0.13	10.36

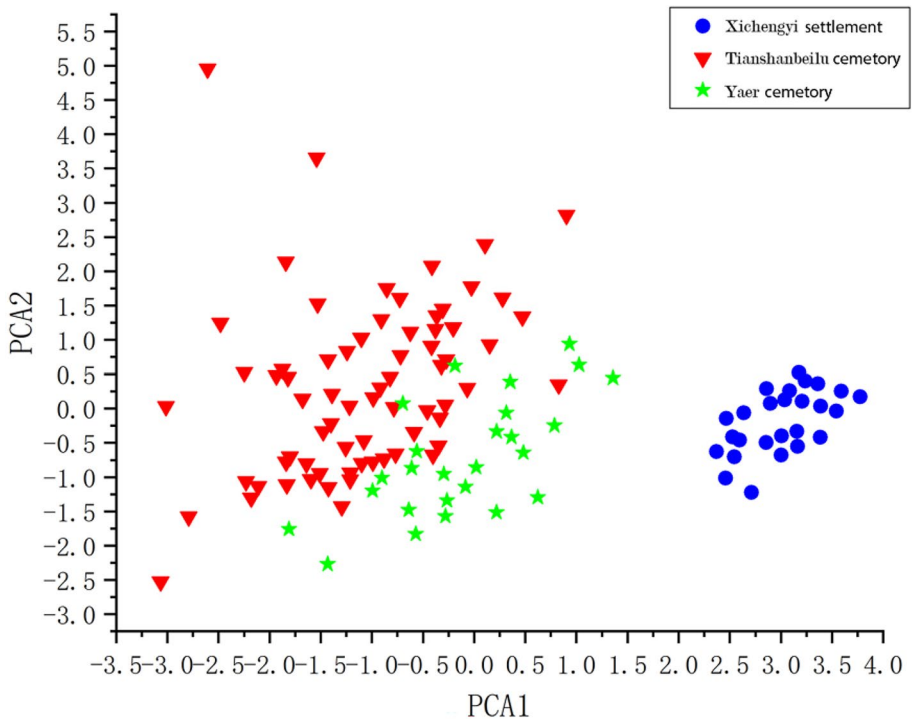

Fig. 9 Chemical compositions of pottery samples from Tianshanbeilu, Yaer, and Xichengyi

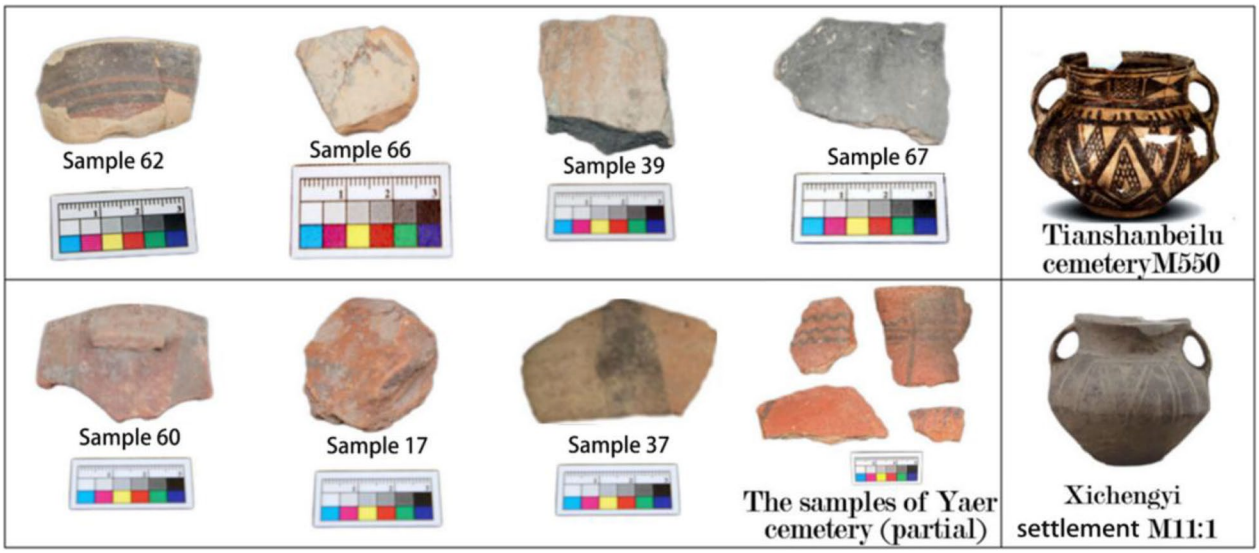

Fig. 10 Comparison of pottery samples from Tianshanbeilu, Yaer cemetery and Xichengyi settlement (Sources of images: M550 from [39]; M11:1 from [40])

not only in the source of raw material but also in the use of reducing kiln.

The compositional characteristics of the pottery samples from Tianshanbeilu partly resonate with those from Yaer but partly diverge from the latter, implying that the populations of the two cemeteries exchanged a part of their pottery wares or shared the same source of clay for production. No overlap occurs with the pottery samples from the Xichengyi settlement, denying the trade of pottery wares between the Hami Basin and the Hexi

Fig. 11 Cross-sectional characteristics of different types of pottery sherds from Tianshanbeilu Cemetery. (① painted red coarse pottery; ② painted yellow coarse pottery; ③ painted red fine pottery; ④&⑤black fine pottery)

Corridor; the similarity of pottery styles is likely derived from technological transmission and cultural diffusion along with population migration. This point, however, has yet to be corroborated with more analyses of pottery samples from other sites of the Machang and Siba cultures in the Hexi Corridor.

Acknowledgements
The authors are indebted to the Xinjiang Institute of Cultural Relics and Archaeology and the Hami Museum for providing samples from pottery ware collection of the archaeological excavation of Tianshanbeilu and Yaer cemetery.

Author contributions
BZ and LZ write and revise the paper; TM provide laboratory equipment and give some useful advices; YW, JZ, and XC provide test pottery samples and give some good writing advices. All authors reviewed the manuscript.

Funding
This work was supported by the Nanjing University Double First-Class Fund (Grant No. 010214914224), the Nanjing University Doctoral Innovation Program (Grant No. CXCY19-04), and the International Collaborative Project Fund.

Data availability
In this work,the original data are shown in Tables 1, 2, 3, and any other further data are available upon request from the authors.

Declarations

Competing interests
The authors have no conflicts of interest to declare that are relevant to the content of this article.

Received: 12 July 2023 Accepted: 20 November 2023
Published online: 11 December 2023

References

1. Lv EG, Chang XE, Wang BH. A brief discussion of Bronze Age Archaeological Culture in Xinjiang. Su Bingqi and Contemporary Chinese Archaeology. Beijing: Science Press; 2001. p. 179–83 (**in Chinese**).
2. Tong JY, Ma J, Li WY, Chang XE, Yu JJ, Wang JX, et al. Chronology of the Tianshanbeilu Cemetery in Xinjiang, Northwestern China. Radiocarbon. 2021;63(1):343–56. https://doi.org/10.1017/RDC.2020.96.
3. Shui T. A comparative study of the bronze age cultures in Xinjiang-with a discussion of the historical process of early Chinese and western cultural exchange. Traditional Chinese studies I. Beijing: Peking University Press; 1993. p. 447–90 (**in Chinese**).
4. Li SC. The collision and exchange of Eastern and Western cultures in the 2nd millennium B.C. as seen from archaeological findings. Xinjiang Cult Relics. 1999;53(1):58–61 (**in Chinese**).
5. Wang TT, Wei D, Chang XE, Yu ZY, Zhang XY, Wang CS, Hu YW, Fuller BT. Tianshanbeilu and the Isotopic Millet Road: reviewing the late Neolithic/Bronze Age radiation of human millet consumption from North China to Europe. Natl Sci Rev. 2019;6(5):1024–39. https://doi.org/10.1093/nsr/nwx015.
6. Gao J, Jin ZY, Wang BH, Chang XE, Wang YQ, Lv EG, Fan AC, Huang F. A provenience study of Bronze Age metal objects from the Hami Basin, Xinjiang, China. J Archaeol Sci Rep. 2021;39: 103175. https://doi.org/10.1016/j.jasrep.2021.103175.
7. Liu C, Liu RL, Zhou PC, Lu C, Yang ZX, Pollard AM, et al. Metallurgy at the crossroads: New analyses of copper-based objects at Tianshanbeilu, eastern Xinjiang, China. Acta Geol Sin English Ed. 2020;94(3):594–602. https://doi.org/10.1111/1755-6724.14531.
8. Gao SZ, Zhang Y, Wei D, Li HJ, Zhao YB, Cui YQ, Zhou H. Ancient DNA reveals a migration of the ancient Di-qiang populations into Xinjiang as early as the early Bronze Age: the Origin Of The Tianshanbeilu Population. Am J Phys Anthropol. 2015;157(1):71–80. https://doi.org/10.1002/ajpa.22690.
9. Rice PM. Pottery analysis: a sourcebook. Chicago and London: University of Chicago press; 2015. p. 349–64.
10. Santacreu DA. Materiality, techniques and society in pottery production the technological study of archaeological ceramics through paste analysis. Berlin: De Gruyter Open Ltd; 2014. p. 194–216.
11. Yu YB, Wu XH, Cui JF, Chen GK, Wang H. Scientific and technological analysis and research of pottery from Xichengye site, Zhangye, Gansu. Archaeology. 2017;829(7):108–20 (**in Chinese**).
12. Geib PR, Callahan MM. Ceramic Exchange within the Kayenta Anasazi Region: Volcanic Ash-Tempered Tusayan White Ware. Kiva. 1987;54(2):95–112. https://doi.org/10.1080/00231940.1987.11758069.
13. Quinn PS. Ceramic petrography: the interpretation of archaeological pottery & related artefacts in thin section. Oxford: Archaeopress; 2003. p. 190–8.
14. Glowacki DM, Neff H, editors. Ceramic production and circulation in the greater Southwest: source determination by INAA and complementary mineralogical investigations. Cotsen Institute of Archaeology at UCLA; 2022. p. 47–66.
15. Stoltman JB. Ceramic petrography and Hopewell interaction. Tuscaloosa: University of Alabama Press; 2015. p. 138–50.
16. Zuo J, Xu CY, Wang CS, Zhang YS. Identification of the pigment in painted pottery from the Xishan site by Raman microscopy. J Raman Spectrosc. 1999;30(12):1053–5. https://doi.org/10.1002/(SICI)1097-4555(199912)30:12%3c1053::AID-JRS473%3e3.0.CO;2-F.
17. Lynch J, Lynch V, Güida JA, Güida JA, Villalba MEC. Pigment identification of prehispanic ceramics during Inka occupation (Catamarca, Argentina) using non-invasive spectroscopy (Infrared-Raman). Vib Spectrosc. 2022;118: 103327. https://doi.org/10.1016/j.vibspec.2021.103327.
18. Bersani D, Lottici PP. Raman spectroscopy of minerals and mineral pigments in archaeometry. J Raman Spectrosc. 2016;47(5):499–530. https://doi.org/10.1002/jrs.4914.
19. Hanson GN. Rare earth elements in petrogenetic studies of igneous systems. Annu Rev Earth Planet Sci. 1980;8(1):371–406. https://doi.org/10.1146/annurev.ea.08.050180.002103.
20. Papageorgiou I. Ceramic investigation: how to perform statistical analyses. Archaeol Anthropol Sci. 2020;12:210. https://doi.org/10.1007/s12520-020-01142-x.
21. Velde B. Composition and mineralogy of clay minerals. Origin and mineralogy of clays: clays and the environment. Berlin: Heidelberg; 1995. p. 8–42.
22. Pollard AM, Heron C. Archaeological chemistry. Cambridge: Royal Society of Chemistry; 2015. p. 98–138.

23. Rye OS. Pottery technology: principles and reconstruction. Manuals on archaeology, No. 4. Washington DC: Taraxacum; 1981.
24. Feng ZS. Petrographic paleogeography of carbonates (in Chinese). Beijing: Petroleum Industry Press; 1989. p. 10–4 (**in Chinese**).
25. Ma QL, Su BM, Hu ZD, Li ZX. Analysis of the composition of pottery excavated from the Dadiwan site in Qin'an, Gansu (in Chinese). Archaeology. 2004;437(2):86–93.
26. Ma HJ, Hein A, Henderson J, Ma QL. The geology of Tianshui-Qin'an area of the western Loess Plateau and the chemical characteristics of its Neolithic pottery. Geoarchaeology. 2020;35(5):611–24. https://doi.org/10.1002/gea.21786.
27. Sendova M, Zhelyaskov V, Scalera M, Ramsey M. Micro-Raman spectroscopic study of pottery fragments from the Lapatsa tomb, Cyprus, ca 2500 BC. J Raman Spectrosc. 2005;36(8):829–33.
28. Zoppi A, Lofrumento C, Castellucci EM, Migliorini MG. The Raman spectrum of hematite: possible indicator for a compositional or firing distinction among Terra Sigillata wares. Annali di Chimica J Anal Environ Cult Herit Chem. 2005;95(3–4):239–46. https://doi.org/10.1002/adic.200590026.
29. Pérez JM, Esteve-Tébar R. Pigment identification in Greek pottery by Raman microspectroscopy. Archaeometry. 2004;46(4):607–14. https://doi.org/10.1111/j.1475-4754.2004.00176.x.
30. Zi J, Büscher H, Falter C, Ludwig W, Zhang KM, Xie XD. Raman shiftsin Si nanocrystals. Appl Phys Lett. 1996;69(2):200–2. https://doi.org/10.1063/1.117371.
31. Post JE, McKeown DA, Heaney PJ. Raman spectroscopy study of manganese oxides: layer structures. Am Miner. 2021;106(3):351–66. https://doi.org/10.2138/am-2021-7666.
32. Sepúlveda M, Gutiérrez S, Vallette MC, Standen VG, Arriaza BT, Cárcamo-Vega JJ. Micro-Raman spectral identification of manganese oxides black pigments in an archaeological context in Northern Chile. Herit Sci. 2015;3:32. https://doi.org/10.1186/s40494-015-0061-2.
33. Rousaki A, Bellelli C, Calatayud MC, Aldazabal V, Custo G, Moens L, Vandenabeele P, Vázquez C. Micro-Raman analysis of pigments from hunter–gatherer archaeological sites of North Patagonia (Argentina). J Raman Spectrosc. 2015;46(10):1016–24. https://doi.org/10.1002/jrs.4723.
34. Liu ZJ, Han YX, Han LG, Cheng YJ, Ma YQ, Fang L. Micro-Raman analysis of the pigments on painted pottery figurines from two tombs of the Northern Wei Dynasty in Luoyang. Spectrochim Acta Part A Mol Biomol Spectrosc. 2013;109:42–6. https://doi.org/10.1016/j.saa.2013.02.015.
35. Chen XF, Ma QL, Zhao GT, Hu ZD, Li ZX. Study on the composite pigments of black and red re-colored pottery of the Banshan and Machang types (in Chinese). J Lanzhou Univ. 2000;36(5):71–6.
36. Li WJ. History of Ancient Chinese Pottery Engineering Technology. Xi'an: Shanxi Education Press; 2017. p. 87–98 (**in Chinese**).
37. Hung LY, Hein A, Womack A. Painted pottery production and social complexity in Neolithic northwest China. Oxford: BAR; 2021. p. 51–137.
38. Zhang LR, Chen JL, Ling Y, Chang XE, Liu GR, Reheman K, Esmayil M, Yan F, Ma Y. Early metallurgy of Eastern Xinjiang. Теория и практика археологических исследований. 2021;33(3):203–39. https://doi.org/10.14258/tpai(2021)33(3).-12.
39. Museum H. The essence of cultural relics in Hami. Beijing: Science Press; 2013. p. 80 (**in Chinese**).
40. Chen GK, Wang H, Li YX, Zhang LR, Yang YG. Xichengyi Site in Zhangye City of Gansu. Archaeology. 2014;641(7):9 (**in Chinese**).

Publisher's Note